Parameterizing Human Locomotion Across Quasi-Random Treadmill Perturbations and Inclines

Rebecca Macaluso, Kyle Embry, *Student Member, IEEE,* Dario J. Villarreal, *Member, IEEE,* and Robert Gregg, *Senior Member, IEEE*

***Abstract*—Previous work has shown that it is possible to use a mechanical phase variable to accurately quantify the progression through a human gait cycle, even in the presence of disturbances. However, mechanical phase variables are highly dependent on the behavior of the body segment from which they are measured, which can change with the human's task or in response to different disturbances. In this study, we compare kinematic parameterization methods based on time, thigh phase angle, and tibia phase angle with motion capture data obtained from ten able-bodied subjects walking at three inclines while experiencing phase-shifting perturbations from a split-belt instrumented treadmill. The belt, direction, and timings of perturbations were quasi-randomly selected to prevent anticipatory action by the subjects and sample different types of perturbations. Statistical analysis revealed that both phase parameterization methods are superior to time parameterization, with thigh phase angle also being superior to tibia phase angle in most cases.**

I. Introduction

THE field of biomechanics has evolved from analyzing human walking offline to measuring and classifying it in real time. Human walking is a repetitive process that is periodic over a gait cycle. A gait cycle consists of a sequence of movements during gait-cycle periods to propel their center of mass forward to achieve locomotion (e.g., heel strike, mid-stance, swing, etc.) [1]. This dissection separates the different locomotor functions of the legs during a gait cycle [2]. In gait analysis, it is important to be able to identify these periods in the gait cycle. Researchers often analyze biomechanical data offline using non-causal signal processing techniques to classify these periods [1]. However, recent technological advances, such as powered prosthetic legs, require measuring the human gait cycle as it happens in real time.

Powered prosthetic legs need to measure the progression of the amputee user's gait cycle in real time to synchronize the prosthetic motion with the user. There are two main methods to measure gait progression in real time: classifying/detecting discrete periods of the gait cycle or measuring the continuous phase of the cycle. The first approach uses sensors on the prosthesis, e.g., force sensors, encoders, and inertial measurement units (IMUs), to detect discrete biomechanical behaviors of the wearer in order to trigger transitions between control modes in a finite state machine control framework [3]. In contrast, real-time estimates of the continuous phase of gait allow the prosthetic leg to track normative joint kinematic patterns in synchrony with the user's motion [4]–[7]. Researchers have used different methodologies (e.g., central pattern generators [8]–[10], oscillators [11]–[13], machine learning [14], extended Kalman filters [15], and phase variables [4]–[7]) to calculate the phase of the gait cycle in a continuous manner. A phase variable is a mechanical signal that increases monotonically with a steady gait cycle and thus can describe the position of a person's kinematics in the gait cycle at all times [5], [16]. When used to control a prosthetic leg, a phase variable gives the user a sense of volitional control over the real-time progression of the prosthetic joints, allowing walking at variable speeds [6] and non-rhythmic behaviors such as starting, stopping, stepping backwards, and kicking [7]. Phase variables have been derived from the global angle of the thigh [6] or tibia [4], which both have sinusoidal trajectories allowing the calculation of a monotonic phase angle from the phase portrait. Although any monotonic signal can parameterize a steady gait cycle, it is important to consider whether the signal predicts the progression of lower-limb joint kinematics during non-steady (e.g., perturbed) gait to control powered prosthetic legs in realistic scenarios.

Studies have used different types of perturbations (e.g., single joint [17]–[22], multi joint [23]–[27], slips [25], [28]–[30], etc.) to understand biomechanical properties of gait including joint impedance [18]–[21], neuromotor control principles [26], [27], [30]–[32], and the robustness of different parameterizations of the gait cycle [29], [33]. In [33] able-bodied subjects walked over a mechatronic platform to induce phase-shifting perturbations at limited onset times of stance (i.e., 100 and 250 ms after initial contact). Motion capture data quantified the ability of a thigh-based phase variable to parameterize the kinematic response of the lower-limb joints to the phase shift in the level-ground gait cycle. The thigh phase variable represented the progression of the hip, knee, and ankle joints significantly better than time across perturbations at the two onset times tested. However, this study did not consider the robustness of the tibia-based phase variable used in [4] or the robustness to different onset times or tasks (e.g., walking

This work was supported by the National Institute of Child Health & Human Development of the NIH under Award Numbers DP2HD080349 and R01HD094772. The content is solely the responsibility of the authors and does not necessarily represent the official views of the NIH. Robert D. Gregg, IV, Ph.D., holds a Career Award at the Scientific Interface from the Burroughs Wellcome Fund.

[1]R. Macaluso is with the Department of Bioengineering, K. Embry is with the Department of Mechanical Engineering, University of Texas at Dallas, Richardson, TX 75080 USA. D. Villarreal is with the Department of Electrical Engineering, Southern Methodist University, Dallas, TX 75205 USA. [2]R. Gregg is with the Department of Electrical Engineering and Computer Science and Robotics Institute, University of Michigan, Ann Arbor, MI 48109, USA. [1]rebecca.macaluso95@gmail.com, [2]rdgregg@umich.edu

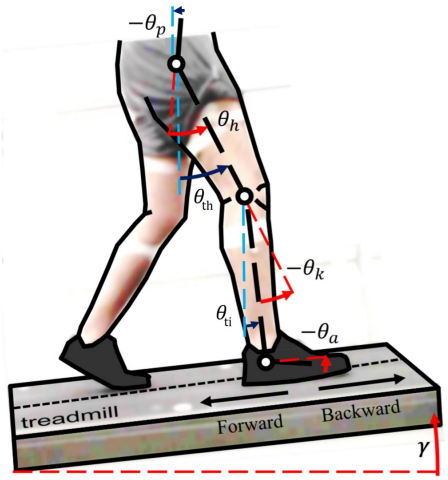

Fig. 1. Diagram of experiment coordinates and angle references. The incline of the treadmill is indicated by γ. The individual joint angles θ_h, θ_k, and θ_a are relative hip, knee, and ankle angles measured with respect to the pelvic tilt, θ_p. The thigh angle θ_{th}, tibia angle θ_{ti} and pelvic tilt are global angles, measured with respect to the gravity vector. The forward and backward arrows indicate how the belt moved the stance foot during each type of perturbation.

on different slopes).

Ground inclination has an effect on hip, knee, and ankle motion during walking [34]–[36]. Since these joints are related to the thigh and tibia angles, they will also be affected by walking at different inclines. Moreover, the kinematic response to perturbations may depend on the onset time due to phase-specific control mechanisms and nonlinear dynamics in gait [37], [38]. *Analyzing the robustness of the previously introduced parameterizations (based on thigh or tibia phase angle) across inclines and quasi-random perturbation times will elucidate whether a single phase variable can be used during varying conditions in powered prosthetic leg applications.*

Section II-C introduces an experimental protocol implemented on a treadmill that exposes able-bodied subjects to phase-shifting perturbations at quasi-random times during the stance period of the subject's gait while walking at different inclines. This protocol addresses limitations of our previous study, such as targeted foot placement, a single level-ground walking task, and limited onset times. Section III-A provides a direct comparison of the robustness of thigh-derived and tibia-derived phase variables, and compares their robustness to traditional time-based parameterization of gait. Section III-B evaluates individual performance of each variable over the different tasks and perturbation types.

II. Methods

A. Definitions

In this study, all kinematic measurements were taken from the sagittal plane with directions and signs for each joint angle illustrated in Figure 1. A "parameterization variable" in the context of this paper is a signal that can be used to predict the angle of the hip, knee, and ankle joints at any point in the gait cycle. This study compared the performance of thigh phase angle, tibia phase angle, and time as parameterization variables, where time is the conventional signal used in gait analysis or trajectory-based control of powered prostheses or orthoses [39]. The first two parameterization variables are respectively calculated in Sections II-D and II-E from the global thigh angle θ_{th}, defined as the angle between the thigh segment and vertical, and the global tibia angle θ_{ti}, defined as the angle between the shank segment and vertical (Figure 1). The robustness of the kinematic parameterizations was evaluated by an experimental protocol using a split-belt treadmill (Bertec, Columbus, OH) to rapidly accelerate/decelerate the belts to effect phase-shifting perturbations to the subject's gait cycle. As shown by the arrows in Figure 1, "forward" perturbations accelerated the progression of the gait cycle by accelerating the stance foot belt along its line of motion, whereas "backward" perturbations delayed the progression of the gait cycle by decelerating, but not stopping, the stance foot belt. An example of how each perturbation direction creates phase shifts in the hip, knee, and ankle joint kinematics can be seen in Figure 2.

B. Programming the Phase-Shifting Perturbations

Velocity profiles were created to induce both forward and backward perturbations on the split-belt treadmill. To execute the desired velocity profile for a perturbation, a series of MATLAB functions from [40] were implemented to remotely control the belts on the treadmill. These functions open and close a TCP/IP communication with the treadmill and read the current velocity of each belt or command a new velocity for each belt. These functions allowed the perturbations to be automated (including the belt, direction, and onset time), rather than created manually by changing the speed with the standard Bertec control software. The treadmill remote control code is available for download as supplemental media [41].

C. Experimental Protocol

The Institutional Review Board at the University of Texas at Dallas approved the experimental protocol described in this section. Ten able-bodied subjects (5 male, age: 25 years $\pm$ 3.4 years, height: 171.6 cm $\pm$ 10.6 cm, weight: 72 kg $\pm$ 10.4 kg) gave written informed consent to participate prior to experimentation. A ten camera motion capture system collected subject kinematic data and measured treadmill belt velocity at 100 Hz (Vicon, Oxford, UK). Force plates underneath each belt of the Bertec instrumented treadmill collected ground reaction forces, moments, and center of pressure.

Subjects self-selected a comfortable speed for walking on level (0° incline), +5° incline, and -5° decline treadmill settings. The order of slopes was randomly assigned to prevent bias from fatigue. Subjects walked at the self-selected speed for a minute without perturbations to produce a control dataset of unperturbed kinematics. From this control data, the average stance time was calculated for each subject to define a normalized time window between 0 and 80% of stance. Then, 100 uniformly distributed times were sampled from this window to determine the perturbation onset times, i.e., the amount of delay between heel strike and perturbation onset. The 80% of stance cutoff marks when the perturbed leg

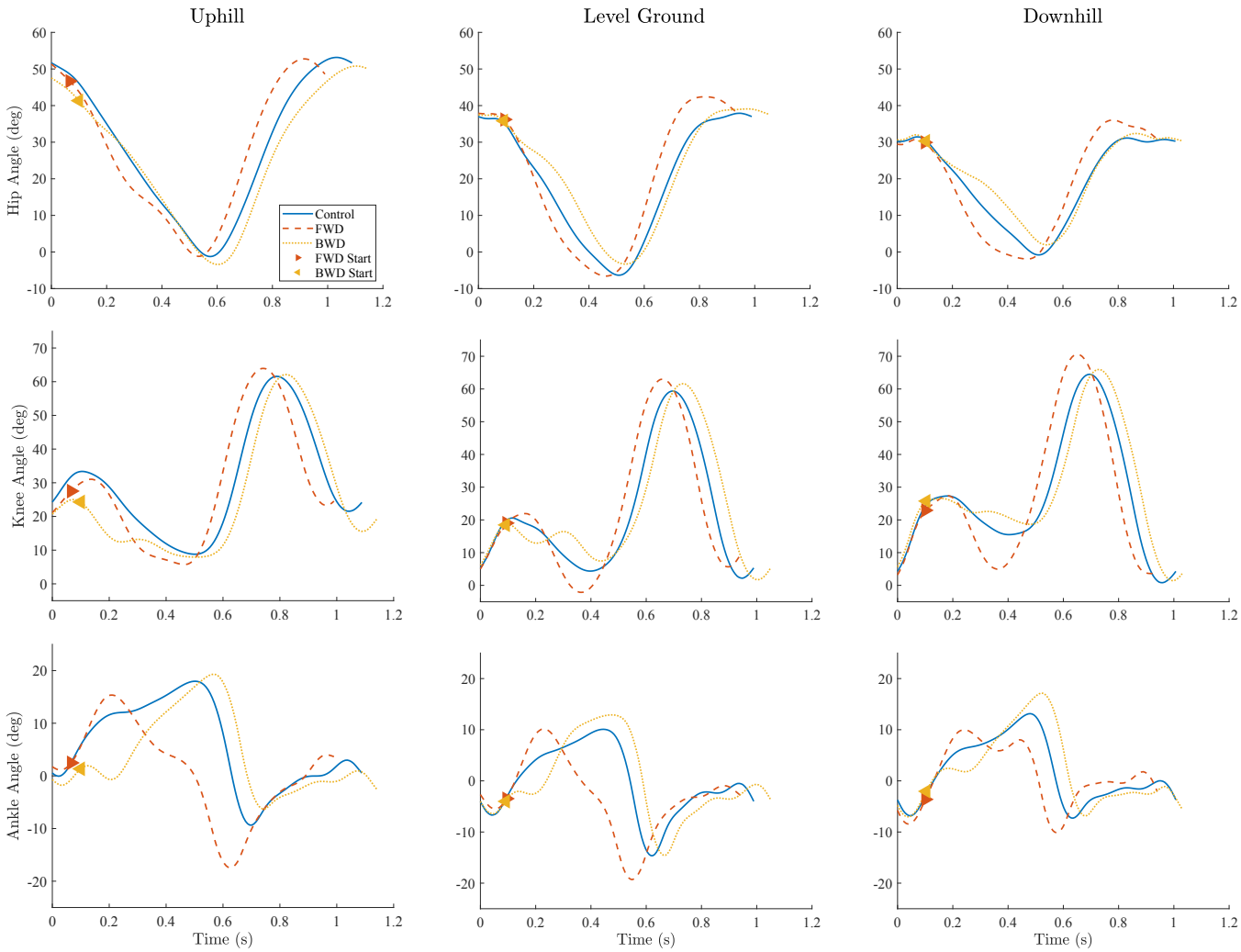

Fig. 2. Example of unperturbed (control) and perturbed joint trajectories of the hip (top), knee (middle), and ankle (bottom) during uphill (left), level-ground (center), and downhill (right) walking. Each plot shows an example of a backward and forward perturbation with the measured onset for each indicated by left facing (yellow) and right facing (red) triangles, respectively.

becomes the trailing leg in double support. Perturbations were not triggered after this point because perturbing the trailing leg in double support does not produce noticeable changes in kinematics [33]. During perturbation trials, subjects walked at the same speed for 20-25 minutes, broken into 5 sets of 4-5 minutes for each slope. A pilot study was conducted to determine desired belt speed for each type of perturbation. Results showed that an 85% difference from the nominal speed could be applied without causing the subject to drastically alter their kinematics. To adjust for overshoot, we programmed perturbations to have a magnitude of 70% difference from the nominal speed. The difference between programmed and measured perturbation profiles is represented in Figure 3. Perturbation onset was randomized in four different ways to prevent anticipatory behavior: 1) the leg to be perturbed was randomly chosen, 2) the direction of the perturbation (forward/backward) was randomized, 3) the number of strides between each perturbation was randomly sampled between 3 to 5 strides, and 4) the order of perturbation onset times was randomized. The number of strides between each perturbation was selected to allow the perturbed and unperturbed leg to re-synchronize [33] as well as give the subject time to relax before reacting to the next perturbation. Subjects experienced a total of 200 perturbations at each incline: 1 forward and 1 backward perturbation at each of the 100 onset times. The number of perturbations to each leg was approximately equal. The collected dataset [41] and video of the perturbations are available for download as supplemental multimedia.

D. Calculating the Thigh Phase Angle

The thigh phase angle derivation begins with the global thigh angle θ_{th} and its time derivative $\dot{\theta}_{\text{th}}$, which is numerically calculated and then filtered with a 5 Hz low-pass cutoff [33]. The global thigh angle and time derivative are then transformed by

$$\begin{aligned} \Theta_{\text{th}}(t) &= -(\theta_{\text{th}} - x_0), \\ \dot{\Theta}_{\text{th}}(t) &= k(\dot{\theta}_{\text{th}} - y_0), \end{aligned} \tag{1}$$

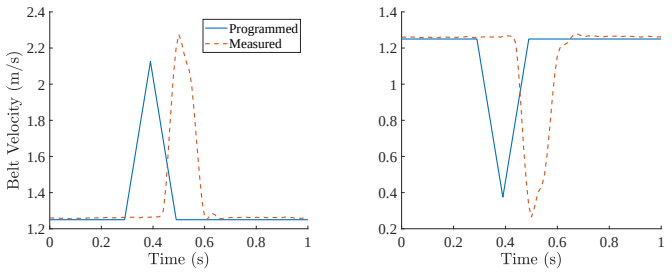

Fig. 3. Plots of programmed and measured treadmill velocity profiles for forward (a) and backward (b) perturbations, averaged across all perturbations from one subject/incline pair.

where the scale factor (k) is chosen to create a more circular phase portrait, and the offsets (x_0 and y_0) center the phase portrait at the origin. These transformations allow the phase variable to approximate a linear function of time and minimize the effect of sensor noise [33]. The scale factor and offsets are computed for each subject and incline condition as

$$k = \frac{|\max(\theta_{\text{th}}) - \min(\theta_{\text{th}})|}{|\max(\dot{\theta}_{\text{th}}) - \min(\dot{\theta}_{\text{th}})|}, \tag{2}$$
$$x_0 = (\max(\theta_{\text{th}}) + \min(\theta_{\text{th}}))/2,$$
$$y_0 = (\max(\dot{\theta}_{\text{th}}) + \min(\dot{\theta}_{\text{th}}))/2,$$

where $\max(\theta_{\text{th}})$, $\min(\theta_{\text{th}})$, $\max(\dot{\theta}_{\text{th}})$, and $\min(\dot{\theta}_{\text{th}})$ are obtained by averaging the maximum and minimum thigh angle and velocity across all strides in the unperturbed control trial. Using control trial data for the offsets and scale factor better simulates the application of this phase variable in powered prostheses, as they would be calculated from previous, unperturbed strides. From [33], the resulting phase variable φ_{th} is given by

$$\varphi_{\text{th}}(t_{\text{i}}) = \left(\text{atan2}(-\dot{\Theta}_{\text{th}}(t_{\text{i}}), \Theta_{\text{th}}(t_{\text{i}})) + \pi\right)/2\pi, \tag{3}$$

where atan2 is the four-quadrant inverse tangent function. We add π to this term and divide by 2π to map the output of atan2 to a range from 0 to 1. If the phase portrait of $\Theta_{\text{th}}(t)$ ever exceeds one full revolution, we add one to the value of $\varphi_{\text{th}}(t_{\text{i}})$ to indicate that the thigh has exceeded the expected trajectory without incurring a heel strike. At heel strike, $\varphi_{\text{th}}(t_{\text{i}})$ is set to exactly zero.

E. Calculating the Tibia Phase Angle

The tibia phase angle is derived in a similar manner from the global tibia angle θ_{ti} and its time derivative $\dot{\theta}_{\text{ti}}$. The phase portrait created when calculating the tibia phase angle is a cardioid-like curve that, when used as an input to Equation 3, creates a monotonic, nonlinear signal as seen in Figure 4. While linearity is not a requirement of a phase variable, it is practically important to maximize linearity to minimize the impact of sensor noise on the predicted joint angles. The scale factor calculated by (2) improves the linearity of the signal, but the non-monotonic trajectory violates a key assumption of a phase variable during steady walking [16]. Due to the unique

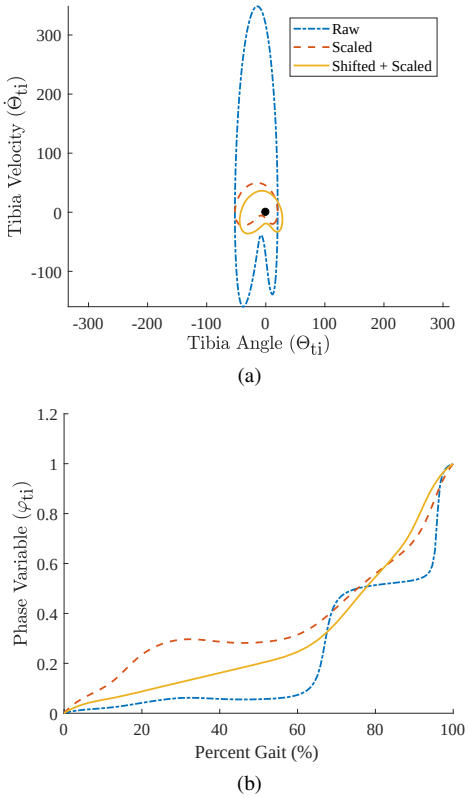

Fig. 4. Plot of phase portrait (a) and resulting phase variable over percent gait (b) for the tibia phase angle scaled by -1 for direction (Raw), scaled by k for direction and linearity (Scaled), and scaled by k and shifted by x_0 and y_0 for direction, linearity, and monotonicity (Shifted+Scaled).

shape of the tibia phase portrait, the calculation of x_0 is altered to align the center of the x-axis to the cusp of the portrait while the equation for y_0 remains the same. The cusp was identified as a local $\dot{\theta}_{\text{ti}}$ maximum between two minima during the first half of the gait cycle. The resulting phase portraits and phase variables can be seen in Figure 4. The corresponding phase variable, φ_{ti}, is calculated using (1) and (3), replacing θ_{th} and $\dot{\theta}_{\text{th}}$ with θ_{ti} and $\dot{\theta}_{\text{ti}}$, respectively. Like the thigh phase angle, we add one to $\varphi_{\text{ti}}(t_{\text{i}})$ if the phase portrait of $\Theta_{\text{ti}}(t)$ exceeds one full revolution and set $\varphi_{\text{ti}}(t_{\text{i}})$ to zero at heel strike.

F. Identifying and Removing Kinematic Outliers

Kinematic outliers among perturbed strides were identified in two different ways. A trip was defined as a perturbed stride with a maximum phase variable greater than 1.3. From the control trials, which contained no perturbations, the largest measured phase variable was 1.12, therefore a cutoff of 1.3 allowed a buffer for perturbed strides. These trips were then manually checked, confirming that the subject could not recover without drastically changing their kinematic pattern. After all trips were removed, the hip, knee, and ankle joints were used to further identify outliers. To ensure similar types of perturbations were compared, onset times were normalized to percent stance, and strides were grouped into four onset phases: initial contact/loading response (IC/LR, 0-20%), mid-stance (21-50%), terminal stance (51-80%), and pre-swing

(81-100%) [2]. Although a time window was used to limit the perturbations in pre-swing, a mechanical delay in the treadmill (as seen in Figure 3) caused a few perturbations to occur during this phase. These groups were used to calculate the mean perturbed trajectory and standard deviation for all joints and onset phases. Individual perturbed strides were then compared to the average perturbed trajectory of the matching onset phase. A stride was marked as an outlier if any joint trajectory exceeded 3 standard deviations away from the corresponding mean perturbed trajectory for at least 10% of the stride. Strides marked as outliers were removed and this process was repeated until no further strides could be removed.

G. Analyzing Parameterizations

The parameterization variables (φ_{th}, φ_{ti}, and time) were each used to parameterize the hip, knee, and ankle of each perturbed stride. A robust parameterization would render the joint kinematics invariant to an ideal phase-shifting perturbation, i.e., the perturbed kinematics match the unperturbed kinematics because the parameterization variable has accounted for the phase shift [33]. To test robustness, the control and perturbed joint angle trajectories were parameterized using each of the three parameterization variables (example in Figure 5). The magnitudes of the parameterized trajectories were then normalized to the range of motion of the average unperturbed trajectory. This was done to minimize the influence of range of motion differences between joints. After normalization, MATLAB was used to calculate the joint-specific correlation coefficient and root mean square error (RMSE) between every perturbed joint trajectory and the average nominal joint trajectory from the control trial. This led to three repeated correlation observations and three repeated RMSE observations at each joint for each perturbation, one for each parameterization variable. Both the correlation coefficient and RMSE were calculated over a complete gait cycle starting with the measured onset of the perturbation, defined as 0%, and ending with the same point in the subsequent unperturbed stride, defined as 100%. This measurement window creates an equal amount of recovery time for each perturbation that allows for a fair comparison between all perturbation timings. To account for variability in the belt velocity signal measured by the motion capture system, the measured onset is defined as the first time the belt velocity exceeded a 1.5% difference from the nominal speed before reaching a local maximum or minimum.

To statistically evaluate the repeated observations, *R* was used to fit the correlation and RMSE of each observation to linear mixed models [42], [43]. Fitting these values to linear mixed models allows for the comparison of repeated data while avoiding problems typically seen with running multiple *t*-tests or repeated measures ANOVA. The dependent variable was correlation in the first model and RMSE in the second model. Since repeated observations from the same subject or from the same physical perturbation event will tend to be highly correlated, the subject and interaction between subject and unique perturbation were treated as random effects. The parameterization variable, stance phase of perturbation onset, perturbation direction, incline, and joint were treated as fixed independent effects. After the data were fit to each model, the mean and 95% confidence interval (CI) were calculated in *R* for each parameterization variable. A pairwise comparison was made using the difference in means between each variable. Adjusting for multiple comparisons, the differences were then tested for statistical significance ($p < 0.05/n, n = 16$).

Six additional models were created to assess the impact of fixed effects on each parameterization variable. For each of the three parameterization variables, a model was created for the resulting correlation or RMSE as the dependent variable. The stance phase of perturbation onset, perturbation direction, incline, and joint were treated as fixed effects, and the subject and interaction between subject and unique perturbation were treated as random effects. In all models, the mean and 95% confidence interval were calculated for each level of each fixed effect. For example, each incline has a mean correlation and 95% confidence interval that is averaged across all other factors.

III. Results

A. Evaluation of Parameterization Variables

Outlier rejection removed 3.61% of the recorded perturbations, leaving $n = 5,609$ for analysis. Figure 6 illustrates the mean correlation and RMSE with 95% CI for each parameterization variable, averaged across all other fixed effects in the model. All correlations are statistically significantly different from each other, with φ_{th} producing the highest correlation, followed by φ_{ti}, then time. All RMSE are statistically significantly different from each other, with φ_{th} producing the lowest RMSE, followed by φ_{ti}, then time. The differences between parameterizations are visualized for an example backward perturbation in Figure 5.

B. Evaluation of Other Fixed Effects

Tables I and II summarize the performance of each parameterization variable across other fixed effects. Table I reports the mean correlation coefficients with lower 95% confidence intervals for each level of each fixed effect, whereas Table II reports the mean RMSE with upper 95% confidence intervals. These confidence intervals reflect that an ideal parameterization will maximize correlation and minimize RMSE.

1) Stance Phase of Perturbation Onset: For perturbations that occurred during initial contact/loading response (IC/LR), mid-stance, and terminal stance phases, the correlation was highest for φ_{th}, followed by φ_{ti} then time. For perturbations that occurred during pre-swing, this order was reversed and time produced the highest correlations while φ_{th} produced the lowest. Looking within each parameterization variable, the correlations for both time and φ_{ti} increased for later onset phases (highest during pre-swing), whereas correlations for φ_{th} were higher when perturbed earlier in the gait cycle.

The RMSE for the four onset phases follows a similar pattern to the correlations, with φ_{th} producing the lowest RMSE and time producing the highest for the first three phases of stance. During pre-swing, this trend is also reversed with time producing the lowest RMSE and φ_{th} producing

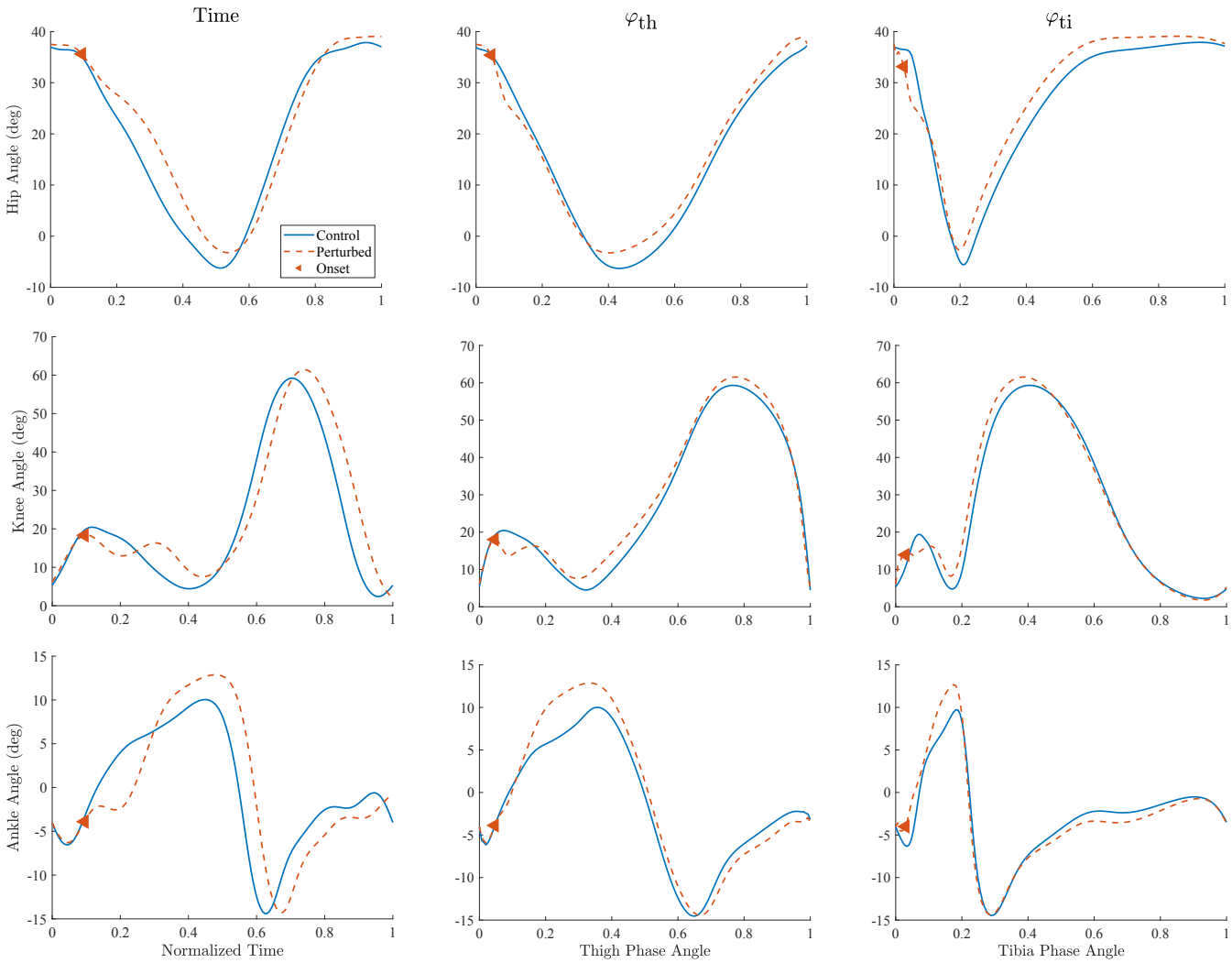

Fig. 5. Example of unperturbed (control) and perturbed joint trajectories of the hip (top), knee (middle), and ankle (bottom) parameterized by time (left), φ_{th} (center), and φ_{ti} (right). The same level-ground, backward perturbation was used for all plots. The measured onset is marked with a left facing triangle.

TABLE I
CORRELATION OF PARAMETERIZATION VARIABLES ACROSS OTHER EFFECTS

Factor	Level	φ_{th}		Time		φ_{ti}	
		Mean	95% CI	Mean	95% CI	Mean	95% CI
Onset Phase	**IC/LR**	0.926	0.887	0.774	0.678	0.837	0.812
	Mid-Stance	0.934	0.895	0.820	0.725	0.861	0.836
	Terminal Stance	0.901	0.863	0.873	0.778	0.869	0.844
	Pre-Swing	0.858	0.736	0.934	0.766	0.895	0.794
Incline	**Uphill (+5°)**	0.931	0.886	0.868	0.771	0.920	0.887
	Level-Ground (0°)	0.918	0.873	0.860	0.763	0.929	0.896
	Downhill (-5°)	0.865	0.820	0.823	0.726	0.748	0.716
Joint	**Hip**	0.960	0.916	0.932	0.835	0.934	0.902
	Knee	0.926	0.881	0.879	0.782	0.948	0.916
	Ankle	0.827	0.783	0.740	0.643	0.714	0.682
Direction	**Backward**	0.898	0.853	0.848	0.751	0.851	0.818
	Forward	0.911	0.867	0.852	0.755	0.881	0.848

TABLE II
RMSE OF PARAMETERIZATION VARIABLES ACROSS OTHER EFFECTS

Factor	Level	φ_{th}		Time		φ_{ti}	
		Mean	95% CI	Mean	95% CI	Mean	95% CI
Onset Phase	**IC/LR**	0.151	0.172	0.238	0.286	0.174	0.189
	Mid-Stance	0.144	0.165	0.211	0.259	0.162	0.177
	Terminal Stance	0.163	0.183	0.173	0.221	0.166	0.181
	Pre-Swing	0.164	0.227	0.129	0.217	0.138	0.197
Incline	**Uphill (+5°)**	0.134	0.158	0.182	0.231	0.133	0.153
	Level-Ground (0°)	0.158	0.182	0.194	0.242	0.133	0.153
	Downhill (-5°)	0.174	0.198	0.188	0.237	0.213	0.233
Joint	**Hip**	0.089	0.113	0.138	0.187	0.123	0.143
	Knee	0.104	0.128	0.125	0.174	0.101	0.121
	Ankle	0.273	0.297	0.300	0.349	0.255	0.274
Direction	**Backward**	0.162	0.186	0.189	0.237	0.168	0.188
	Forward	0.149	0.173	0.187	0.236	0.151	0.171

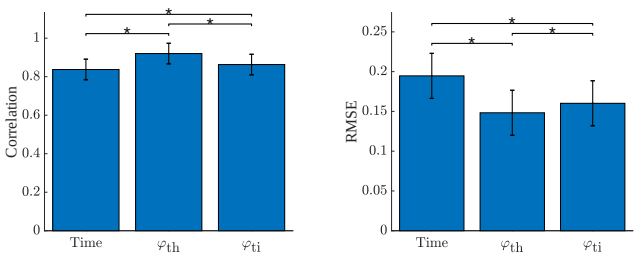

Fig. 6. Mean correlation (a) and RMSE (b) for each parameterization variable with 95% CI, averaged across all other fixed effects. Asterisk denotes statistically significant difference.

the highest RMSE. The correlation trend seen in each phase variable is also present in RMSE, with φ_{th} producing lower RMSE during early stance and φ_{ti} and time producing lower RMSE during late stance.

2) Incline: The correlation produced by φ_{th} and time was highest for perturbations that occurred during uphill walking, followed by level-ground and then downhill walking. Similarly, the correlation produced by φ_{ti} was lowest for perturbations during downhill walking. However, it was highest for perturbations during level-ground walking rather than uphill walking.

The RMSE produced by φ_{th} and φ_{ti} was lowest for perturbations during uphill walking, followed by level-ground and then downhill walking. For time, RMSE was lowest for perturbations during uphill walking and highest for level-ground walking.

Figure 7 contains the average unperturbed thigh and tibia phase portraits for each incline, the resulting phase variables, and their derivatives. In the thigh phase portraits (Figure 7a), both uphill and level-ground walking complete one full revolution while the downhill phase portrait appears to double back on itself. As seen in Figure 7b, φ_{th} monotonically increases for both uphill and level-ground walking, whereas the downhill case appears to decrease slightly around heel strike. This change in direction is confirmed by the derivative of φ_{th} dipping below 0 at the beginning and end of the stride during downhill walking (Figure 7c). The tibia phase portraits (Figure 7d) have similar shapes for all inclines, with the uphill case having a slightly smaller radius than the other cases. In Figure 7e, φ_{ti} for each incline increases monotonically, as confirmed by Figure 7f. However, the trajectories for φ_{th} appear more linear than those of φ_{ti}.

3) Joint: The correlation produced by φ_{th} and time was highest when parameterizing the hip joint, followed by the knee then ankle. For φ_{ti}, the highest correlation results from parameterizing the knee, followed by hip then ankle. The RMSE produced by φ_{th} was lowest when parameterizing the hip, followed by the knee then ankle. For time and φ_{ti}, RMSE was the lowest when parameterizing the knee, followed by the hip then the ankle.

4) Direction: Within each perturbation direction, φ_{th} produces the highest correlation followed by φ_{ti} then time. The RMSE for each direction follows an analogous pattern with φ_{th} producing the lowest, followed by φ_{ti} then time. For each parameterization variable, forward perturbations result in higher correlation and lower RMSE when compared to results from backward perturbations.

IV. DISCUSSION

A. Evaluation of Parameterization Variables

The results of Figure 6 show that across different perturbation conditions and inclines, parameterizing joints with φ_{th} produced the highest correlation and lowest RMSE when compared to an unperturbed joint trajectory. This means that, out of the variables studied, φ_{th} was the most accurate parameterization variable, followed by φ_{ti} and time. Both phase angles appear viable for controlling powered prostheses, where φ_{th} may be more practical for an above-knee prosthesis [6] and φ_{ti} may be more practical for a below-knee prosthesis [4].

B. Evaluation of Other Fixed Effects

1) Stance Phase of Perturbation Onset: Tables I and II show that onset time had an effect on the performance of the parameterization variables studied. Specifically, both φ_{th} and φ_{ti} are noticeably better than time (higher correlation, lower RMSE) for initial contact/loading response, mid-stance, and terminal stance phases (0% - 80% stance). During pre-swing, the trend is reversed with time producing higher correlation and lower RMSE than both phase variables. We believe that these trends relate to the loading/unloading of weight on the

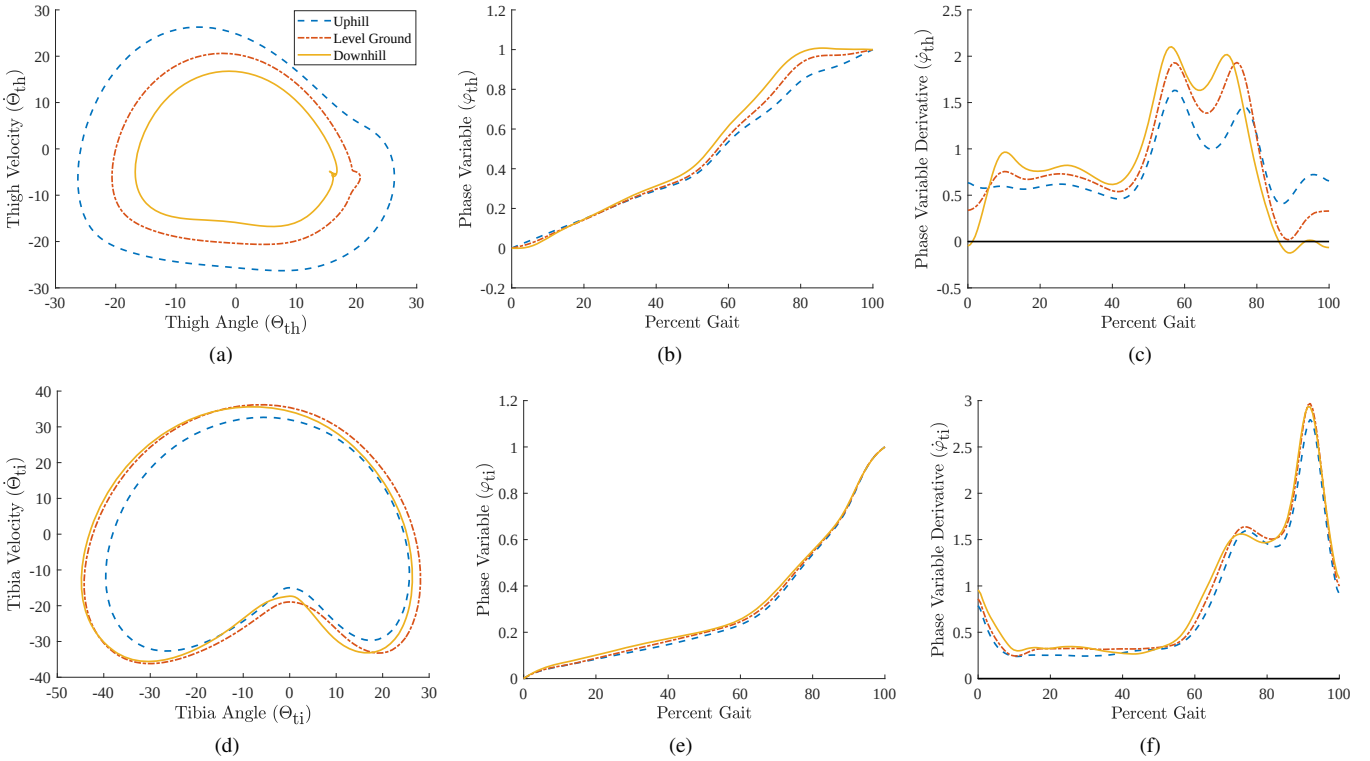

Fig. 7. Plots of the phase portrait created by the thigh (a) and tibia (b), the resulting phase variables (c-d), and their derivatives (e-f) at each walking incline averaged across all subjects.

perturbed leg during each phase. In initial contact/loading response, the main task of the leg is weight acceptance, meaning the perturbed leg is being loaded. In mid-stance and terminal stance, the main task is single limb support on the perturbed leg. By the time the leg reaches pre-swing, however, the opposite leg has begun its weight acceptance and the perturbed leg is being unloaded. This implies that phase variables are better suited for controlling phases where weight is loaded onto the leg and time is better suited for controlling phases where weight is unloaded from the leg.

2) Incline: The results of Tables I and II indicate that φ_{th} and φ_{ti} performed better with uphill and level-ground walking than with downhill walking. This trend may relate back to desirable properties of phase variables as defined in [33]. One of the criteria for a phase orbit to provide a viable phase variable candidate is that the unwrapped signal is monotonically increasing or decreasing. The lack of monotonicity in the downhill case of Figure 7c could explain why φ_{th} did not perform as well for downhill perturbations, but this does not explain the change in performance for φ_{ti}, which is monotonic at all inclines. Time also performed best during uphill walking but had decreased performance for both downhill and level-ground walking. The observed trends are likely related to differences in the kinematic response to perturbations when walking at different inclines. The perturbation effect may have been more significant when walking at level ground or downhill, resulting in greater deviations from the nominal trajectory regardless of the parameterization.

3) Joint: Tables I and II show that φ_{th} provides the best parameterization (i.e., highest correlation and lowest RMSE) for the hip joint and φ_{ti} provides the best parameterization for the knee. This trend is to be expected because φ_{th} is derived from the hip joint while φ_{ti} is derived from the knee joint. For the ankle, φ_{th} had the highest correlation and φ_{ti} had the lowest RMSE. All three parameterizations produced relatively lower correlations and higher RMSE for the ankle compared to the knee and the hip. This can be attributed to the ankle being closest to the belt-driven perturbations and thus more impacted than the proximal joints. All of these findings are illustrated in the different parameterizations of the perturbation response in Figure 5.

4) Direction: The results of Tables I and II show that direction is the only factor where all parameterization variables follow the same trend: higher correlations and lower RMSE for forward perturbations than backward perturbations. This could be attributed to how each type of perturbation affects the time spent in stance and swing phases of gait. In forward perturbations, the foot is advanced through the stance phase while backward perturbations delay the foot's progress. This difference results in strides with forward perturbations having more time in swing than their backward counterparts, creating the trend seen in all parameterization methods.

C. Limitations and Future Work

While this study analyzes phase variable performance at varying slopes and walking speeds, it is assumed that the walking incline is not measured in real time. Investigating

a way to measure and incorporate the walking slope into the phase variable calculation could lead to more consistent performance across inclines. Another limitation of this study is that it focused on steady-state tasks, but did not analyze non-steady tasks like starting, stopping, and turning. In [7], a piecewise holonomic phase variable was introduced that was robust during periodic walking as well as starting and stopping on level-ground. Future work will include further investigation of phase variable improvements, evaluation of non-steady tasks, and inclusion of a piecewise holonomic phase variable.

V. Conclusion

This paper analyzed the effectiveness of time, the thigh phase angle, and the tibia phase angle as parameterization variables for a variety of environmental circumstances that impact human walking. While ground inclination, perturbation direction, and perturbation timing all have measurable effects on parameterization accuracy, a statistical analysis shows that both thigh and tibia phase angles are better parameterization variables than time in most cases. Although the thigh phase angle was statistically better than the tibia phase angle, the latter may be more practical for controlling a powered ankle prosthesis or ankle-foot orthosis. In those instances, our results still support the use of the tibia phase angle as a robust phase variable for the controller.

Acknowledgements

The authors would like to acknowledge S. Zalsha from the Department of Statistical Science at Southern Methodist University for her consulting services in determining the appropriate statistical analyses for this study.

References

[1] D. A. Winter, *Biomechanics and motor control of human movement*. Hoboken, NJ: John Wiley & Sons, 2009.

[2] J. Perry and J. Burnfield, *Gait analysis: normal and pathological function*, 2nd ed. Thorofare, NJ: Slack Incorporated, 2010.

[3] F. Sup, A. Bohara, and M. Goldfarb, "Design and control of a powered transfemoral prosthesis," *The International journal of robotics research*, vol. 27, no. 2, pp. 263–273, 2008.

[4] M. A. Holgate, T. G. Sugar, and A. W. Bohler, "A novel control algorithm for wearable robotics using phase plane invariants," in *IEEE International Conference on Robotics and Automation*, vol. 14, no. 3, 2009, pp. 3845–3850.

[5] D. J. Villarreal and R. D. Gregg, "A survey of phase variable candidates of human locomotion," in *IEEE Engineering in Medicine and Biology Conf.*, 2014, pp. 4017–4021.

[6] D. Quintero, D. J. Villarreal, D. J. Lambert, S. Kapp, and R. D. Gregg, "Continuous-phase control of a powered knee–ankle prosthesis: Amputee experiments across speeds and inclines," *IEEE Transactions on Robotics*, vol. 34, no. 3, pp. 686–701, 2018.

[7] S. Rezazadeh, D. Quintero, N. Divekar, E. Reznick, L. Gray, and R. D. Gregg, "A phase variable approach for improved rhythmic and non-rhythmic control of a powered knee-ankle prosthesis," *IEEE Access*, vol. 7, pp. 109 840–109 855, 2019.

[8] F. Dzeladini, J. Van Den Kieboom, and A. Ijspeert, "The contribution of a central pattern generator in a reflex-based neuromuscular model," *Frontiers in human neuroscience*, vol. 8, p. 371, 2014.

[9] R. J. Vogelstein, R. Etienne-Cummings, N. V. Thakor, and A. H. Cohen, "Phase-dependent effects of spinal cord stimulation on locomotor activity," *IEEE Transactions on Neural Systems and Rehabilitation Engineering*, vol. 14, no. 3, pp. 257–265, 2006.

[10] I. A. Rybak, N. A. Shevtsova, M. Lafreniere-Roula, and D. A. McCrea, "Modelling spinal circuitry involved in locomotor pattern generation: insights from deletions during fictive locomotion," *The Journal of physiology*, vol. 577, no. 2, pp. 617–639, 2006.

[11] A. Taghvaei, H. S. A, and P. G. Mehta, "A coupled oscillators-based control architecture for locomotory gaits," in *53rd IEEE Conference on Decision and Control*, Dec 2014, pp. 3487–3492.

[12] R. Ronsse, N. Vitiello, T. Lenzi, J. Van Den Kieboom, M. C. Carrozza, and A. J. Ijspeert, "Human–robot synchrony: flexible assistance using adaptive oscillators," *IEEE Transactions on Biomedical Engineering*, vol. 58, no. 4, pp. 1001–1012, 2010.

[13] A. K. Tilton, E. T. Hsiao-Wecksler, and P. G. Mehta, "Filtering with rhythms: Application to estimation of gait cycle," in *American Control Conference*. IEEE, 2012, pp. 3433–3438.

[14] I. Kang, P. Kunapuli, and A. J. Young, "Real-time neural network-based gait phase estimation using a robotic hip exoskeleton," *IEEE Transactions on Medical Robotics and Bionics*, 2019.

[15] N. Thatte, T. Shah, and H. Geyer, "Robust and adaptive lower limb prosthesis stance control via extended kalman filter-based gait phase estimation," *IEEE Robotics and Automation Letters*, vol. 4, no. 4, pp. 3129–3136, 2019.

[16] E. R. Westervelt, J. W. Grizzle, C. Chevallereau, J. H. Choi, and B. Morris, *Feedback Control of Dynamic Bipedal Robot Locomotion*. CRC Press, 2007.

[17] V. Dietz, G. Colombo, and R. Müller, "Single joint perturbation during gait: neuronal control of movement trajectory," *Experimental Brain Research*, vol. 158, pp. 308–316, 2004.

[18] H. Lee, P. Ho, M. Rastgaar, H. I. Krebs, and N. Hogan, "Multivariable static ankle mechanical impedance with active muscles," *IEEE Transactions on Neural Systems and Rehabilitation Engineering*, vol. 22, no. 1, pp. 44–52, 2013.

[19] H. Lee and N. Hogan, "Time-varying ankle mechanical impedance during human locomotion," *IEEE Transactions on Neural Systems and Rehabilitation Engineering*, vol. 23, no. 5, pp. 755–764, 2014.

[20] M. R. Tucker, A. Moser, O. Lambercy, J. Sulzer, and R. Gassert, "Design of a wearable perturbator for human knee impedance estimation during gait," in *IEEE International Conference on Rehabilitation Robotics*, 2013, pp. 1–6.

[21] E. Rouse, L. Hargrove, E. Perreault, and K. T. Peshkin Michael, "Development of a mechatronic platform and validation of methods for estimating ankle stiffness during the stance phase of walking," *Journal of Biomechanical Engineering*, vol. 135, no. 8, 2013.

[22] M. Vlutters, E. H. Van Asseldonk, and H. van der Kooij, "Foot placement modulation diminishes for perturbations near foot contact," *Frontiers in bioengineering and biotechnology*, vol. 6, p. 48, 2018.

[23] Y.-C. Pai and T. S. Bhatt, "Repeated-slip training: an emerging paradigm for prevention of slip-related falls among older adults," *Physical therapy*, vol. 87, no. 11, pp. 1478–1491, 2007.

[24] J. van Doornik and T. Sinkjær, "Robotic platform for human gait analysis," *IEEE transactions on biomedical engineering*, vol. 54, no. 9, pp. 1696–1702, 2007.

[25] P. Parijat and T. E. Lockhart, "Effects of moveable platform training in preventing slip-induced falls in older adults," *Annals of biomedical engineering*, vol. 40, no. 5, pp. 1111–1121, 2012.

[26] J. K. Moore, S. K. Hnat, and A. J. van den Bogert, "An elaborate data set on human gait and the effect of mechanical perturbations," *PeerJ*, vol. 3, p. e918, 2015.

[27] R. C. Sheehan, E. J. Beltran, J. B. Dingwell, and J. M. Wilken, "Mediolateral angular momentum changes in persons with amputation during perturbed walking," *Gait & posture*, vol. 41, no. 3, pp. 795–800, 2015.

[28] C. A. Haynes and T. E. Lockhart, "Evaluation of gait and slip parameters for adults with intellectual disability," *Journal of biomechanics*, vol. 45, no. 14, pp. 2337–2341, 2012.

[29] D. J. Villarreal, D. Quintero, and R. D. Gregg, "A Perturbation Mechanism for Investigations of Phase-Dependent Behavior in Human Locomotion," *IEEE Access*, vol. 4, pp. 893–904, 2016.

[30] D. Yoo, K.-H. Seo, and B.-C. Lee, "The effect of the most common gait perturbations on the compensatory limbs ankle, knee, and hip moments during the first stepping response," *Gait & posture*, vol. 71, pp. 98–104, 2019.

[31] V. Dietz, G. Horstmann, and W. Berger, "Interlimb coordination of leg-muscle activation during perturbation of stance in humans," *Journal of neurophysiology*, vol. 62, no. 3, pp. 680–693, 1989.

[32] J. Skidmore and P. Artemiadis, "Unilateral floor stiffness perturbations systematically evoke contralateral leg muscle responses: a new approach

to robot-assisted gait therapy," *IEEE Transactions on Neural Systems and Rehabilitation Engineering*, vol. 24, no. 4, pp. 467–474, 2015.

[33] D. J. Villarreal, H. A. Poonawala, and R. D. Gregg, "A robust parameterization of human gait patterns across phase-shifting perturbations," *IEEE Trans. Neural Syst. Rehabil. Eng.*, vol. 25, no. 3, pp. 265–278, 2016.

[34] A. Leroux, J. Fung, and H. Barbeau, "Postural adaptation to walking on inclined surfaces: I. normal strategies," *Gait & posture*, vol. 15, no. 1, pp. 64–74, 2002.

[35] A. N. Lay, C. J. Hass, and R. J. Gregor, "The effects of sloped surfaces on locomotion: a kinematic and kinetic analysis," *Journal of biomechanics*, vol. 39, no. 9, pp. 1621–1628, 2006.

[36] K. R. Embry, D. J. Villarreal, R. L. Macaluso, and R. D. Gregg, "Modeling the kinematics of human locomotion over continuously varying speeds and inclines," *IEEE transactions on neural systems and rehabilitation engineering*, vol. 26, no. 12, pp. 2342–2350, 2018.

[37] J. M. Donelan and K. G. Pearson, "Contribution of sensory feedback to ongoing ankle extensor activity during the stance phase of walking," *Canadian journal of physiology and pharmacology*, vol. 82, no. 8-9, pp. 589–598, 2004.

[38] V. Dietz and J. Duysens, "Significance of load receptor input during locomotion: a review," *Gait & posture*, vol. 11, no. 2, pp. 102–110, 2000.

[39] M. R. Tucker, J. Olivier, A. Pagel, H. Bleuler, M. Bouri, O. Lambercy, J. del R Millán, R. Riener, H. Vallery, and R. Gassert, "Control strategies for active lower extremity prosthetics and orthotics: a review," *Journal of neuroengineering and rehabilitation*, vol. 12, no. 1, p. 1, 2015.

[40] P. Iturralde, "HMRL-Matlab-Treadmill-Functions," 2013. [Online]. Available: https://github.com/willpower2727/HMRL-Matlab-Treadmill-Functions

[41] R. Macaluso, K. Embry, D. Villarreal, and R. D. Gregg, "Human kinematics, kinetics, and EMG during phase-shifting perturbations at varying inclines," *IEEE DataPort*, 2020, http://dx.doi.org/10.21227/12hp-e249.

[42] B. T. West, K. B. Welch, and A. T. Galecki, *Linear mixed models: a practical guide using statistical software*. Chapman and Hall/CRC, 2014.

[43] R Core Team, *R: A Language and Environment for Statistical Computing*, R Foundation for Statistical Computing, Vienna, Austria, 2018. [Online]. Available: https://www.R-project.org/